Chapter 2

Vehicle Dynamics Modeling

This chapter provides information on dynamics modeling of vehicle and tire. The vehicle axis system used throughout the simulation is according to the SAE standard, as described in SAE J670e [18]. According to a brief research study of typical vehicle models, a nonlinear three-degree-of-freedom vehicle model will be used in this research. The derivation of that model including the tire model is discussed first. The equations of motion are then converted to a state space form for ease of integration and a Third Order Runge-Kutta integration routine is used as the integration algorithm. Finally, the vehicle model is verified against results from Smith et al. [14] to show its validity.

2.1 Vehicle Axis System

Throughout this thesis, the coordinate system used in vehicle dynamics modeling will be according to SAE J670e [18] as shown in Figure 2.1. The x-axis points to the forward direction or the longitudinal direction, the y-axis, which represents the lateral direction, is positive when it points to the right of the driver, and the z-axis points to the ground satisfying the right hand rule.
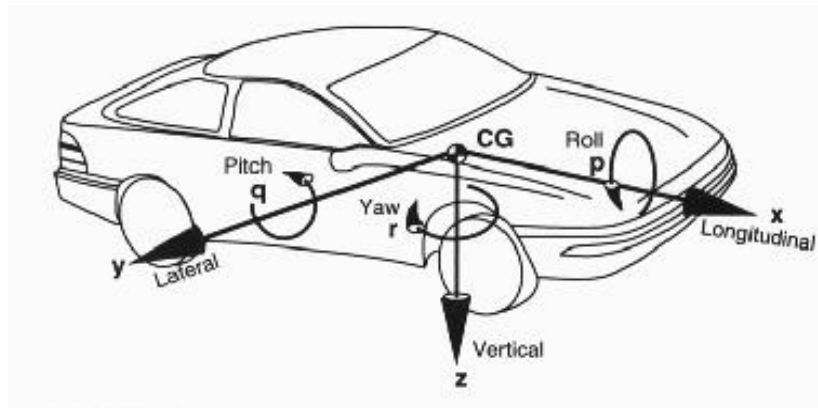

Figure 2.1 Vehicle Axis System after SAE [18]

In most studies related to handling and directional control, only the X-Y plane of the vehicle is considered. The vertical axis, Z, is often used in the study of ride, pitch, and roll stability type problems. The following list defines relevant definitions for the variables associated with this research.

Longitudinal direction: forward moving direction of the vehicle. There are two different ways of looking at the forward direction, one with respect to the vehicle body itself, and another with respect to a fixed reference point. The former is often used when dealing with acceleration and velocity of the vehicle. The latter is used when the location information of the vehicle with respect to a starting or an ending point is desired.

Lateral direction: sideways moving direction of the vehicle. Again, there are two ways of looking at the lateral direction, with respect to the vehicle and with respect to a fixed reference point. Researchers often find this direction more interesting than the longitudinal one since extreme values of lateral acceleration or lateral velocity can decrease vehicle stability and controllability.

Tire slip angle: This is equivalent to heading in a given direction but walking at an angle to that direction by displacing each foot laterally as it is put on the ground as shown in Figure 2.2. The foot is displaced laterally due to the presence of lateral forces.
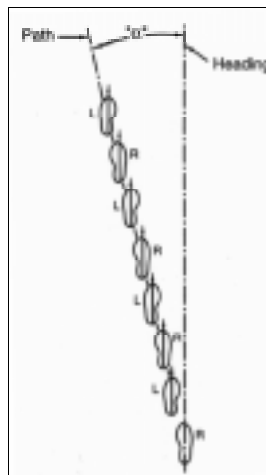

Figure 2.2 Walking Analogy to Tire Slip Angle after Milliken [19]

Figure 2.3 shows the standard tire axis system that is commonly used in tire modeling. It shows the forces and moments applied to the tire and other important parameters such as slip angle, heading angle, etc.
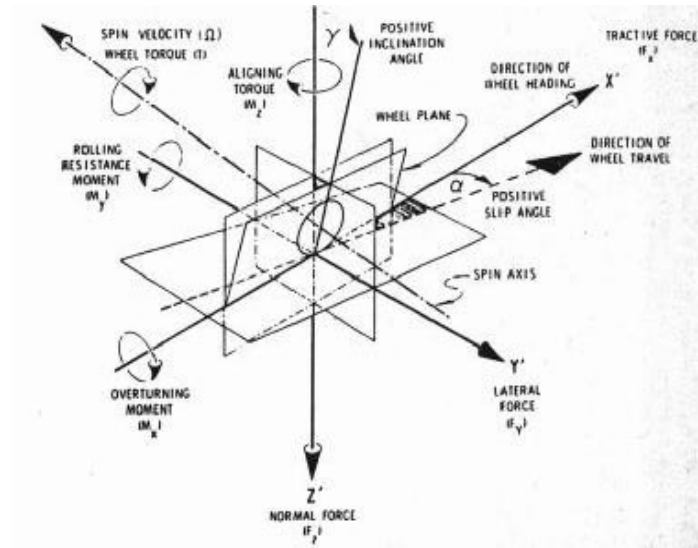

Figure 2.3 SAE Tire Axis System after Milliken [19]

Body-slip angle: is the angle between the X-axis and the velocity vector that represents the instantaneous vehicle velocity at that point along the path, as shown in Figure 2.4. It should be emphasized that this is different from the slip angle associated with tires. Even though the concept is the same, each individual tire may have different slip angle at the same instant in time. Often the body slip angle is calculated as the ratio of lateral velocity to longitudinal velocity.

Figure 2.4 Body-Slip Angle after Milliken [19]
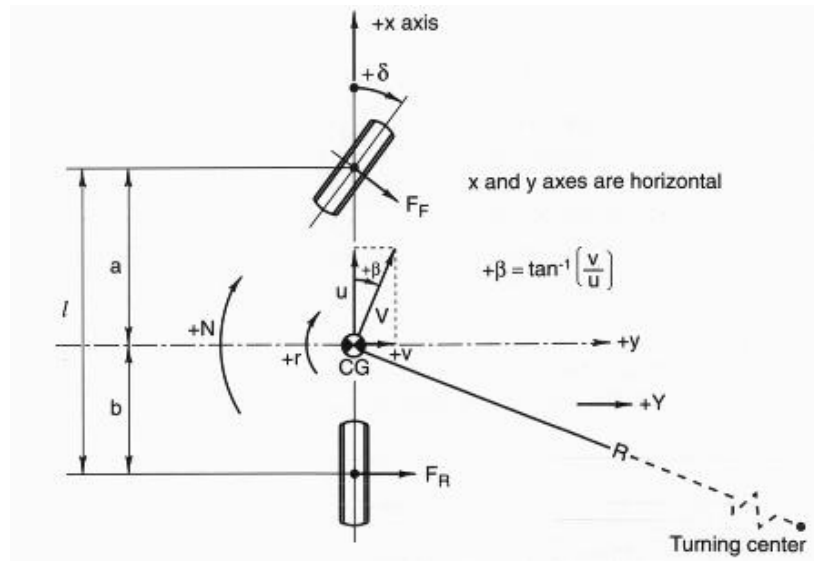
In order to simplify the vehicle model so that results of the integration can be quickly calculated, the effects of camber angle, load transfer, and aerodynamics are not included in this study.

2.2 Vehicle Models

There are numerous degrees of freedom associated with vehicle dynamics. The most simplified vehicle dynamic model is a two-degree-of-freedom bicycle model, representing the lateral and yaw motions. The idea behind this model is that sometimes it is not necessary or desirable to include the longitudinal direction, because it does not affect the lateral or yaw stability of the vehicle. This model, which is easier to understand, is often used in teaching purposes. Figure 2.5 shows the two-degree-of-freedom model.
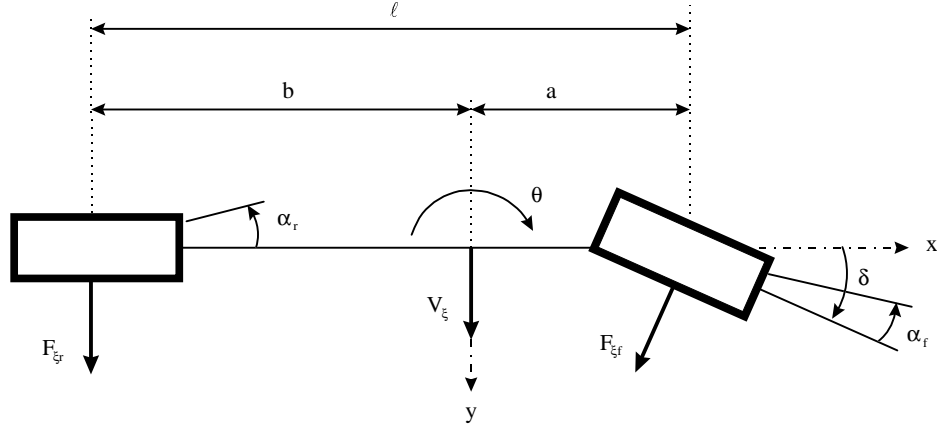
Figure 2.5 Two-Degree-of-Freedom Model

A three-degree-of-freedom model adds longitudinal acceleration to the model, therefore enabling one to describe the full vehicle motion in the X-Y plane. As shown in Figure 2.6, the longitudinal velocity, U, and the longitudinal force, F_{tf} and F_{tr}, are included into the model. This is the model that is used throughout this research.
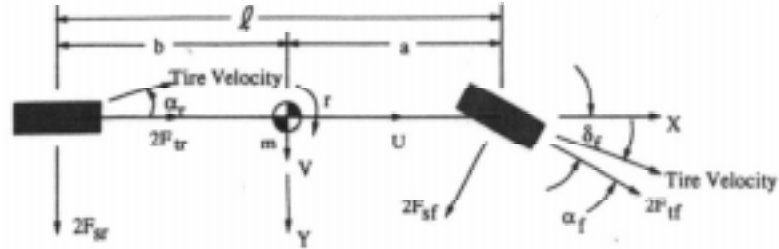

Figure 2.6 Three-Degree-of-Freedom Model after Smith [18]

In some studies, the rotational degrees of freedom for the front and rear wheels are added to the model to include the effects of longitudinal slip, as shown in Figure 2.7. This five-degree-of freedom model enables one to perform an in-depth study of traction and braking forces on handling maneuvers by including the effects of wheel spin. Rotational degrees of freedom are also often used in the studies of combined braking and steering, and braking system controller design, [2,20].
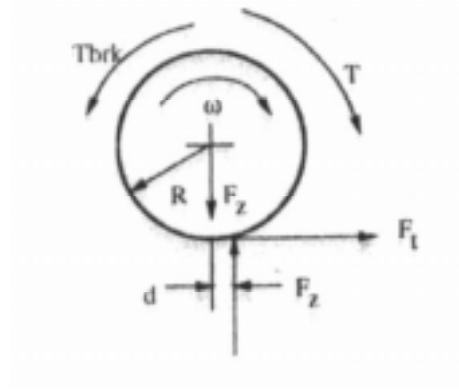
14

Figure 2.7 Rotational Degree of Freedom at Wheel after Smith [18]

An eight-degree-of-freedom model no longer assumes symmetry in dynamic behavior between right and left sides. Rotational degree of freedom for each of the four tires is considered in this vehicle model instead of two tires. It also adds a rolling motion, ϕ_s, between left and right sides of the vehicle. This model is often used in the suspension design or ride comfort analysis, specifically looking at the effects of these issues with respect to roll and side-to-side load transfer.
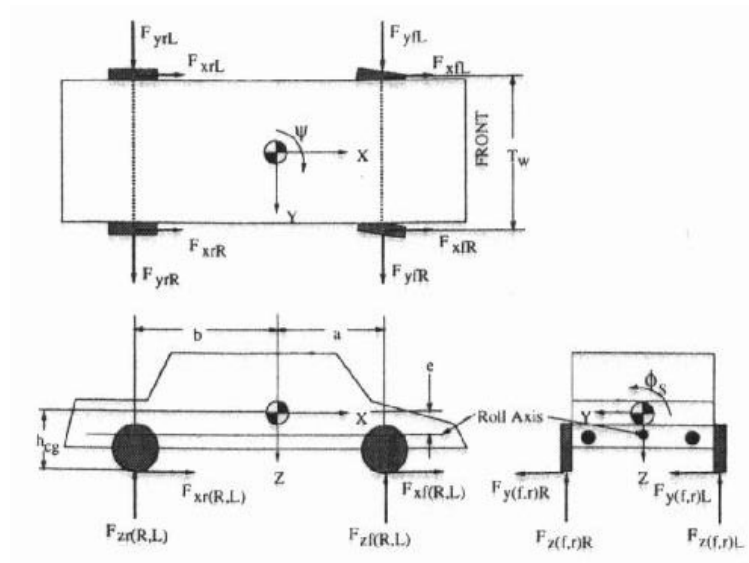

Figure 2.8 Eight-Degree of Freedom Model after Smith [18]

2.3 Three-Degree-of-Freedom Vehicle Model Derivation

Capturing all the motions of a vehicle into analytical equations can be quite difficult. Although including more number of elements in the model may increase the model's accuracy, it substantially increases the computation time. This section describes the derivation of the three-degree-of-freedom bicycle model used in this study. It also includes the equations for the front and rear tire slip angles. For this research this is the first step in the process, before proceeding to designing an optimization algorithm. This section of the chapter also describes concepts such as tire slip angle, friction ellipse, longitudinal force limits, and state space representation.

2.3.1 Equations of Motion

The three degrees of freedom model considered for this study is governed by the following equations:

$$I\ddot{\theta} = aP_f\delta + bF_{\xi f} - bF_{\xi r} \tag{2.1}$$

$$m(\dot{V}_\xi + V_\eta\dot{\theta}) = P_f\delta + F_{\xi f} + F_{\xi r} \tag{2.2}$$

$$m(\dot{V}_\eta + V_\xi\dot{\theta}) = P_f + P_r + F_{\xi f}\delta \tag{2.3}$$

Referring to Figure 2.9, the lateral and longitudinal velocities of the vehicle with respect to the fixed coordinate system XYZ can be described as shown in Eqs. (2.4) and (2.5).
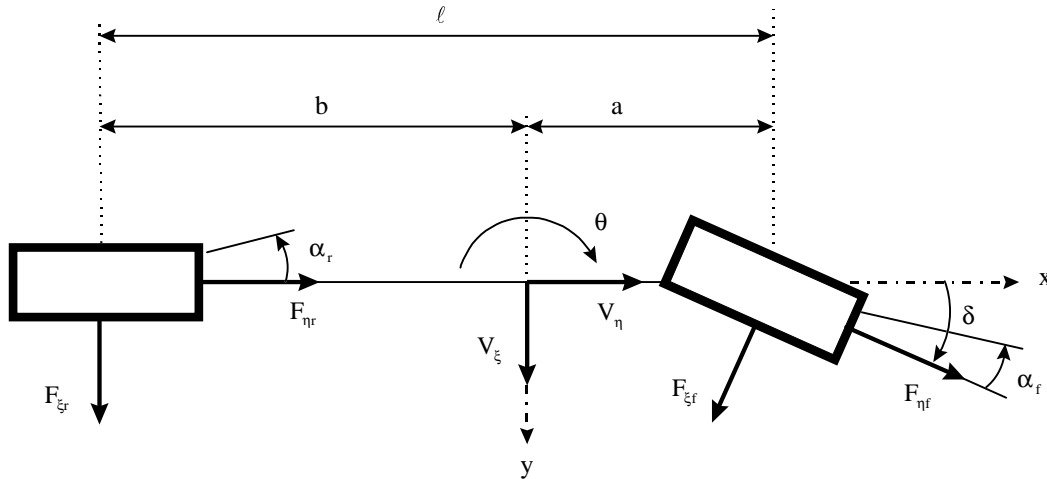

Figure 2.9 Three-Degree-of-Freedom Used for Simulation

$$\dot{x} = -V_\xi \sin\theta + V_\eta \cos\theta \tag{2.4}$$

$$\dot{y} = V_\xi \cos\theta + V_\eta \sin\theta \tag{2.5}$$

Where

$F_{\xi f}, F_{\xi r}$ = lateral tire force on front and rear tires

a   = vehicle center of gravity location from front axle

b   = vehicle center of gravity location from rear axle

m   = vehicle mass

I   = vehicle yaw inertia

P_f, P_r = longitudinal force on front and rear tires

V_η, V_ξ = longitudinal/lateral velocity of vehicle in body reference frame

x, y   = longitudinal/lateral position of vehicle in inertial reference frame

δ = steering angle

η = longitudinal axis in body reference frame

θ = yaw angle

ξ = lateral axis in body reference frame

The parameters used for the simulation are shown in Table 1. These parameters are based on vehicle specifications provided by The Goodyear Tire and Rubber Company [21].

Table 2.1 Vehicle Parameter Used for Simulation Study

Property	Value
Mass	1292.2 kg
Inertia (about Z-axis)	2380.7 kgm^2
Front Axle to Center of Gravity	1.006 m
Rear Axle to Center of Gravity	1.534 m
Height Center of Gravity Location	0.3 m

2.3.2 Front Tire Slip Angle Derivation

Front tire slip angle is a function of front tire steering angle, the longitudinal velocity vector, the lateral velocity vector, and the lateral velocity component due to yaw. Figure 2.10 illustrates the front tire slip angle, which is mathematically defined as

$$\alpha_f = \delta - \frac{\left(a\dot{\theta} + V_\xi\right)}{V_\eta} \tag{2.6}$$

where

δ = steering angle

a = center of gravity location from vehicle rear axle

θ = yaw velocity of vehicle

V_ξ = lateral velocity of vehicle

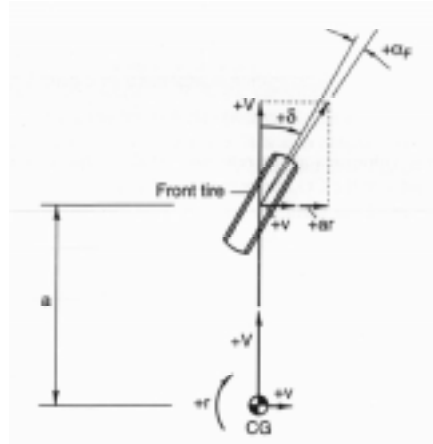V_η = longitudinal velocity of vehicle

Figure 2.10 Front Tire Slip Angle after Milliken [19]

Equation (2.6), which describes the front tire slip angle formula, assumes that the slip angle is small. It is necessary to determine the front tire slip angle because the Segel lateral force tire model is a function of slip angle [7]. This tire model will be explained in details in a later section. The Segel lateral force model will be discussed in Section 2.5.

18

2.3.3 Rear Tire Slip Angle Derivation

The rear tire slip angle is a result of a combination of the ratio of the longitudinal velocity vector and the lateral velocity vector, and the lateral velocity component due to yaw. Figure 2.11 illustrates the rear tire slip angle.

$$\alpha_r = \frac{\left(b\dot{\theta} - V_\xi\right)}{V_\eta} \tag{2.7}$$

where

b = center of gravity location from vehicle rear axle

θ = yaw velocity of vehicle

V_ξ = lateral velocity of vehicle

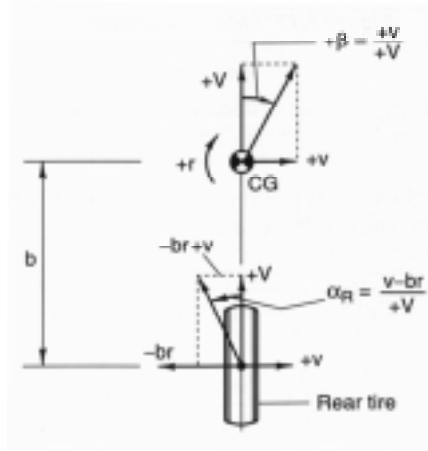V_η = longitudinal velocity of vehicle

Figure 2.11 Rear Tire Slip Angle after Milliken [19]

Equation (2.7), which describes the rear tire slip angle formula, assumes that the slip angle is small. It is necessary to determine the rear tire slip angle because the Segel lateral force tire model is a function of slip angle [7]. This tire model will be explained in details in a later section. The Segel lateral force model will be described in Section 2.5.

2.4 Longitudinal (Traction/Braking) Force

The traction force limit for a front wheel drive vehicle is calculated as the following, [22].

$$F_{x\,max,t} = \frac{\mu\dfrac{Wb}{l}}{1+\mu\dfrac{h}{l}} \qquad (2.8)$$

The maximum braking force for an independent suspension, front wheel drive vehicle is calculated as the following, [22].

$$F_{x\,max,b} = \mu\frac{W}{l}(a+\mu h) \qquad (2.9)$$

where

$F_{x\,max,t}$ = maximum tractive force
$F_{xmax.b}$ = maximum braking force
μ = friction coefficient
a = center of gravity location from front axle
b = center of gravity location from rear axle
W = vehicle weight
l = vehicle wheelbase
h = center of gravity location from ground

The values of Eq. (2.8) and (2.9) are calculated to be 5913.73 N and -5349.33 N respectively, using the parameters in Table 1. Throughout this study, however, the traction force limit and the braking force limit are set to 5000 N and -5000 N, respectively. This enables the use of one variable to describe the constraint of the longitudinal force in the optimal control algorithm. This is explained in more details in Chapter 3.

20

2.5 Segel Lateral Force Model

There are several lateral force models that have been derived in the past. They range from using a collective set of tire performance data, to determining an empirical lateral force model, to analytical tire models derived from differential equations describing the deformation of tire structure [7]. The lateral force model selected for this research is the Segel Model. This model was developed in the early 1970's. There are newer models that can be used to describe the lateral force of a tire. However, Segel model is fairly easy to use and has relatively small computation time [7]. It is a function of the slip angle, cornering stiffness, tire vertical load, friction coefficient, and longitudinal force, as described below.

$$F_{\xi i} = \mu F_{zi}\left(\tilde{\alpha}_i - \frac{\tilde{\alpha}_i|\tilde{\alpha}_i|}{3} + \frac{\tilde{\alpha}_i^{\,3}}{27}\right)\sqrt{\left(1 - \frac{P_i^{\,2}}{\mu^2 F_{zi}^2} + \frac{P_i^{\,2}}{c_i^{\,2}}\right)} \qquad i = f, r \qquad (2.10)$$

$$\tilde{\alpha}_i = \frac{c_i \alpha_i}{\mu F_{zi}} \qquad i = f, r \qquad (2.11)$$

$$\alpha_f = \delta - \frac{\left(a\dot{\theta} + V_\xi\right)}{V_\eta} \qquad (2.12)$$

$$\alpha_r = \frac{\left(b\dot{\theta} - V_\xi\right)}{V_\eta} \qquad (2.13)$$

$$F_{zf} = \frac{mgb - \left(P_f + P_r\right)h}{a + b} \qquad (2.14)$$

$$F_{zr} = \frac{mga + \left(P_f + P_r\right)h}{a + b} \qquad (2.15)$$

where

$$c_f, c_r = \text{cornering stiffness of front and rear tires}$$
$$F_{zf}, F_{zr} = \text{normal tire load on front and rear tires}$$
$$F_{\xi f}, F_{\xi r} = \text{lateral tire force on front and rear tires}$$
$$g = \text{gravitational acceleration}$$
$$h = \text{height of the center of gravity}$$
$$a = \text{front axle to center of gravity distance}$$
$$b = \text{rear axle to center of gravity distance}$$
$$m = \text{vehicle mass}$$
$$\mu = \text{friction coefficient}$$
$$\alpha_f, \alpha_r = \text{slip angle of front and rear tires}$$
$$P_f, P_r = \text{longitudinal force of front and rear tires}$$
$$V_\xi, V_\eta = \text{longitudinal \& lateral velocity in body reference frame}$$
$$x, y = \text{longitudinal \& lateral position in inertial reference frame}$$
$$\delta = \text{steering angle}$$
$$\theta = \text{yaw angle}$$
$$\dot{\theta} = \text{yaw velocity}$$

2.6 Friction Ellipse Concept

This topic is discussed in this section because it is related to the two previous topics, longitudinal force and lateral force. The friction circle concept is actually used in the optimization portion of the research as a part of the cost function, which attempts to maximize the tire forces.
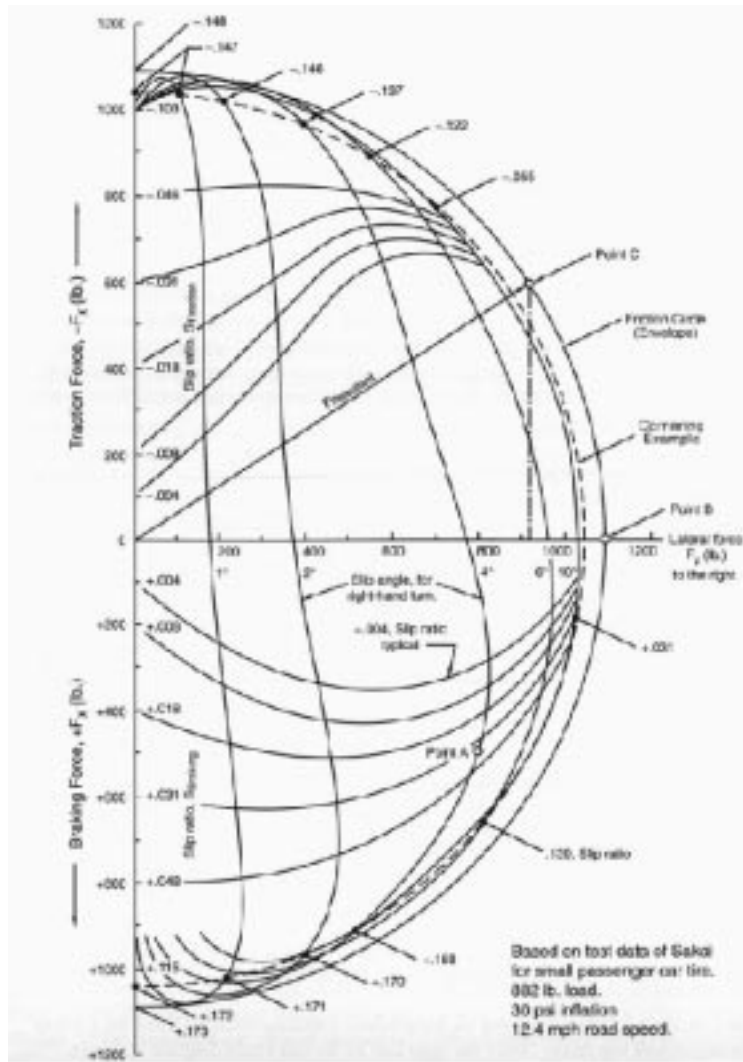
Figure 2.12 Friction Ellipse Diagram after Milliken [19]

Figure 2.12 illustrates a friction ellipse. The diagram combines the longitudinal force, which is a function of slip ratio, and the lateral force, which is a function of slip angle into one plot. The elliptical shape represents the limits of longitudinal and lateral forces due to friction. Inside this ellipse, one can look up the nominal longitudinal force at a certain slip ratio, knowing the slip angle and lateral force, and vice versa. A shortcoming of the friction ellipse diagram is that the information is only specific to a certain load, tire pressure and temperature. Numerous diagrams are necessary to fully describe the performance of the tire.

2.7 Friction Circle Concept

Friction circle is a simplified version of the friction ellipse. The limit, which is shown as a circle in Figure 2.13, is defined by the product of friction coefficient of the road and the vertical load of the vehicle on that tire. This friction model does not take into account slip angle and slip ratio. This is convenient for this research because it does not require extensive tire data with respect to various slip ratios, slip angles, and loads.
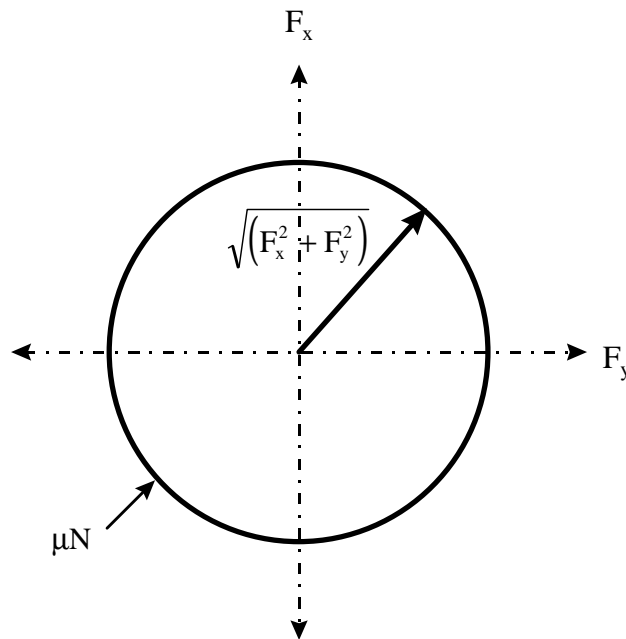

Figure 2.13 Friction Circle Diagram

2.8 Equations of Motion Solution

The three-degree-of-freedom vehicle model equations of motion must be rewritten in first order differential equations, to enable using the first-order numerical integration method, such as the third order Runge-Kutta, which was used in this study.

The state space representation of the dynamic equations in (2.1) - (2.5) is,

$$\dot{x}_1 = \frac{\left(aP_f\delta + bF_{\xi f} - bF_{\xi r}\right)}{I} \tag{2.16}$$

$$\dot{x}_2 = \frac{\left(P_f\delta + F_{\xi f} + F_{\xi r}\right)}{m} - x_3 x_1 \tag{2.17}$$

$$\dot{x}_3 = \frac{\left(P_f + P_r - F_{\xi f}\delta\right)}{m} - x_2 x_1 \tag{2.18}$$

$$\dot{x}_4 = -x_2 \sin x_6 + x_3 \cos x_6 \tag{2.19}$$

$$\dot{x}_5 = x_2 \cos x_6 + x_3 \cos x_6 \tag{2.20}$$

$$\dot{x}_6 = x_1 \tag{2.21}$$

where

$x_1 = \dot{\theta}$ yaw rate

$x_2 = V_\xi$ lateral velocity

$x_3 = V_\eta$ longitudinal velocity

$x_4 = x$ longitudinal position with respect to fixed reference

$x_5 = y$ lateral position with respece to fixed reference

$x_6 = \theta$ yaw angle

There are numerous integration routines that can be used to integrate the state space equations [15]. Two criteria for selecting which integration routine to use are the computation time and accuracy of the results. One such method is the Runge-Kutta routine, which has an accuracy of a Taylor series integration method without requiring the calculation of higher derivatives. The Runge-Kutta method itself has up to five levels of accuracy where the higher the order the more accurate the integration results will be. The trade-offs in selecting which order to use are the difficulty of algorithm implementation and computation time. After careful consideration of different routines, the third order Runge-Kutta routine was selected [15].

2.9 Vehicle Model Validation

The three-degree-of-freedom vehicle model used in this study is validated against a known source, a study by Smith et al. [14]. There are two types of steering input

subjected by the vehicle model, saw-tooth and step. Figure 2.14 shows the saw-tooth steering input and the vehicle response corresponding to that input. Figure 2.15 shows response of the three-degree-of-freedom model.
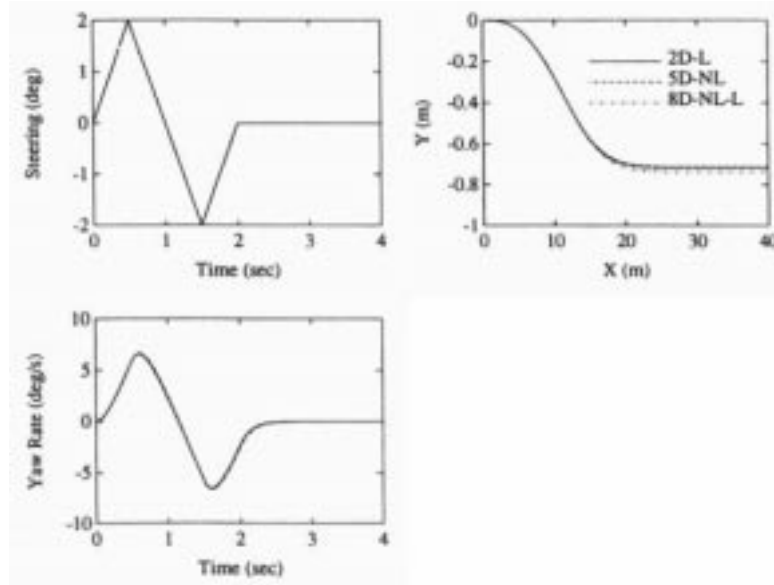

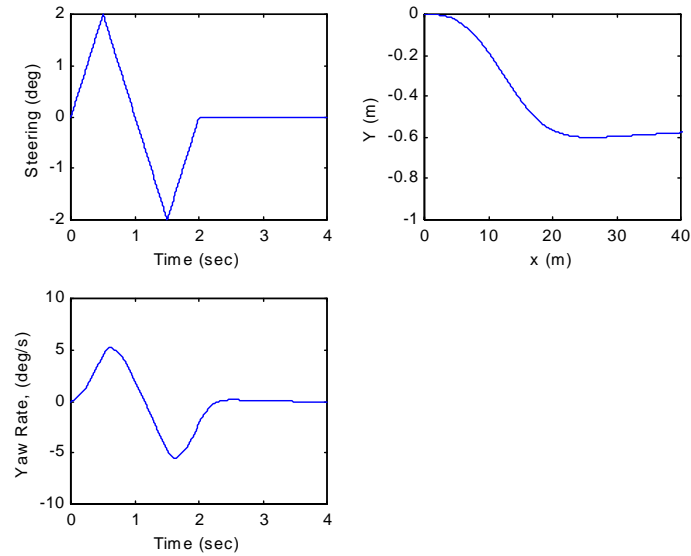**Figure 2.14 Smith Vehicle Response with Saw-Tooth Input after Smith [14]**

Figure 2.15 Three-Degree-of-Freedom Model Response Subjected to Saw-Tooth Input

The vehicle model is also validated against the step input from Smith's study. Figure 2.16 shows the step input and the vehicle response according to that input. Figure 2.17 shows the three-degree-of-freedom model response subjected to the same input.
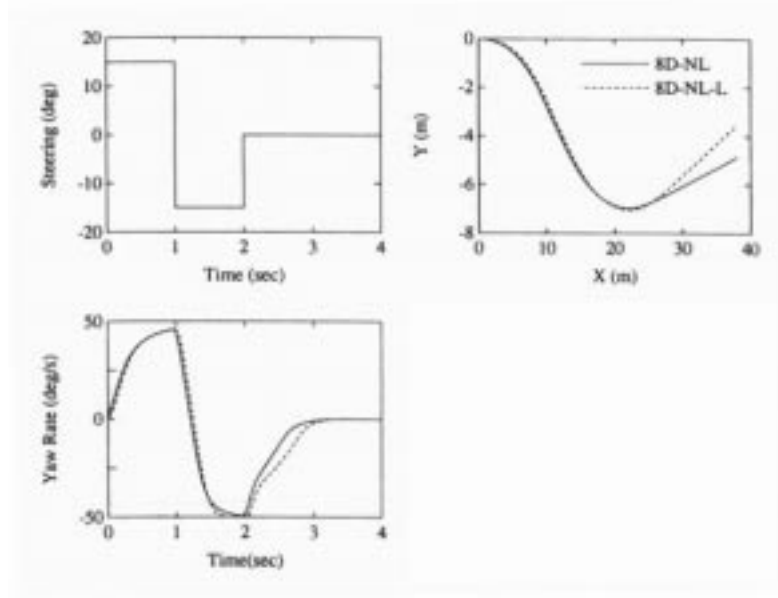

Figure 2.16 Smith Vehicle Response with Step Input after Smith [14]
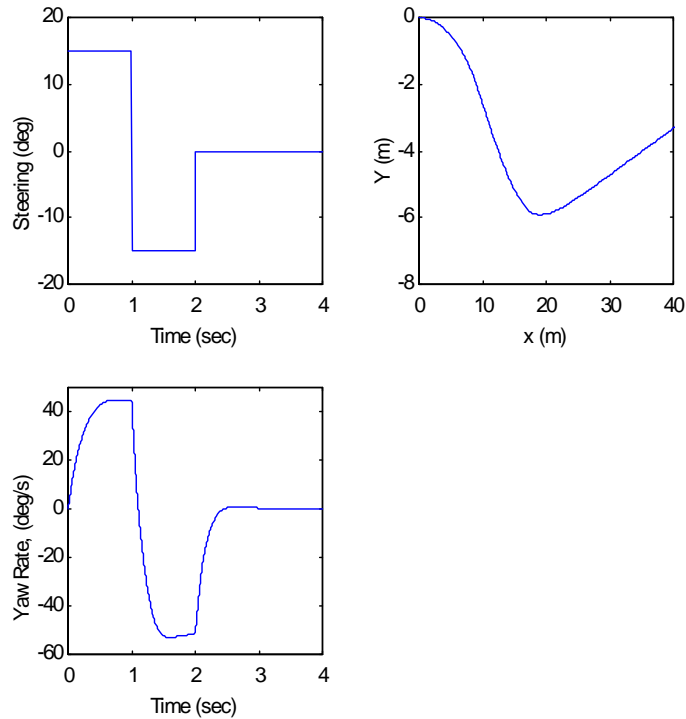

Figure 2.17 Three-Degree-of-Freedom Model Response Subjected to Step Input

It can be concluded that the three-degree-of-freedom model is valid since the response of this model closely follows the response generated by Smith. Therefore, the vehicle model of this study is concluded to be acceptable and valid.